

(21) Application No: 0700653.9
(22) Date of Filing: 12.01.2007

(51) INT CL:
B01F 13/00 (2006.01) B01L 3/00 (2006.01)
G01N 27/447 (2006.01)

(71) Applicant(s):
Brunel University
(Incorporated in the United Kingdom)
UXBRIDGE, Middlesex, UB8 3PH,
United Kingdom
(continued on next page)

(56) Documents Cited:
EP 1658890 A2 EP 1462174 A1
WO 2006/004558 A1 WO 2003/057368 A1
US 20020036141 A1

(58) Field of Search:
INT CL B01F, B01J, B01L, B03C, B81B, F04B, G01N
Other: Online: WPI & EPODOC

(54) Abstract Title: A Microfluidic device

(57) A microfluidic device for mixing comprises an inlet 30, 32, and three layers 12, 22, and 24. The first layer 12 comprises first 1 and second 2 current carrying structures, wherein the first and second current carrying structures each comprise a plurality of teeth 14, 16, 18, and wherein the teeth of the first and second current carrying structures are offset such that the teeth of the first current carrying structure are positioned between the teeth of the second current carrying structure. The second layer comprises a first microfluidic chamber 22 in fluid communication with the inlet 30, 32 positioned above the first and second current carrying structures of the first layer. The third layer comprises a third and fourth current carrying structures wherein the third 3 and fourth 4 current carrying structures each comprise a plurality of teeth, and the teeth of the third and fourth current carrying structures are offset such that the teeth of the third current carrying structure are positioned between the teeth of the fourth current carrying structure. The third and fourth current carrying structures are positioned in the third layer so as to be above the first microfluidic chamber and such that the teeth of the third current carrying structure are positioned substantially vertically above or offset from the teeth of the first current carrying structure and the teeth of the fourth current carrying structure are positioned substantially vertically above or offset from the teeth of the second current carrying structure. The teeth have a stem having a substantially elliptical tip 40. The microfluidic device uses the magnetic field produced by the conductors to move paramagnetic beads disposed in the fluid and is particularly used in association with blood based biological samples and PCR amplification systems.

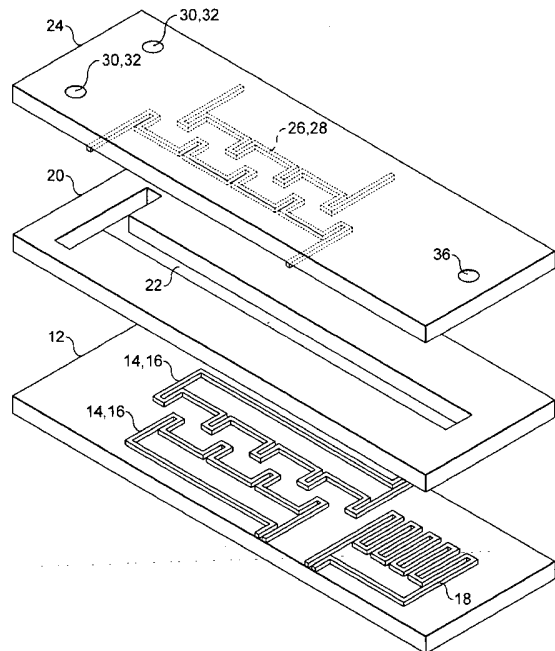


FIG. 1

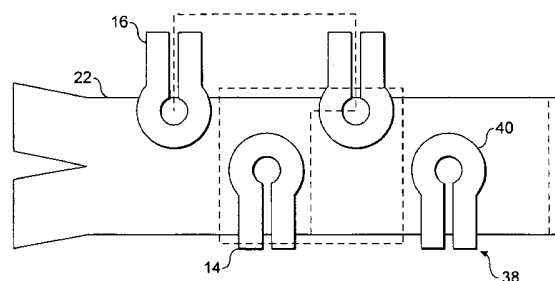


FIG. 2

GB 2446204 A continuation

(72) Inventor(s):

**Wamadeva Balachandran
Sayad Mohamad Azimi
Jeremy Clive Ahern
Massoud Zolgharni
Mohamed Reza Bahmanyar
Predrag Slijepcevic**

(74) Agent and/or Address for Service:

**Boult Wade Tennant
Verulam Gardens, 70 Gray's Inn Road,
LONDON, WC1X 8BT, United Kingdom**

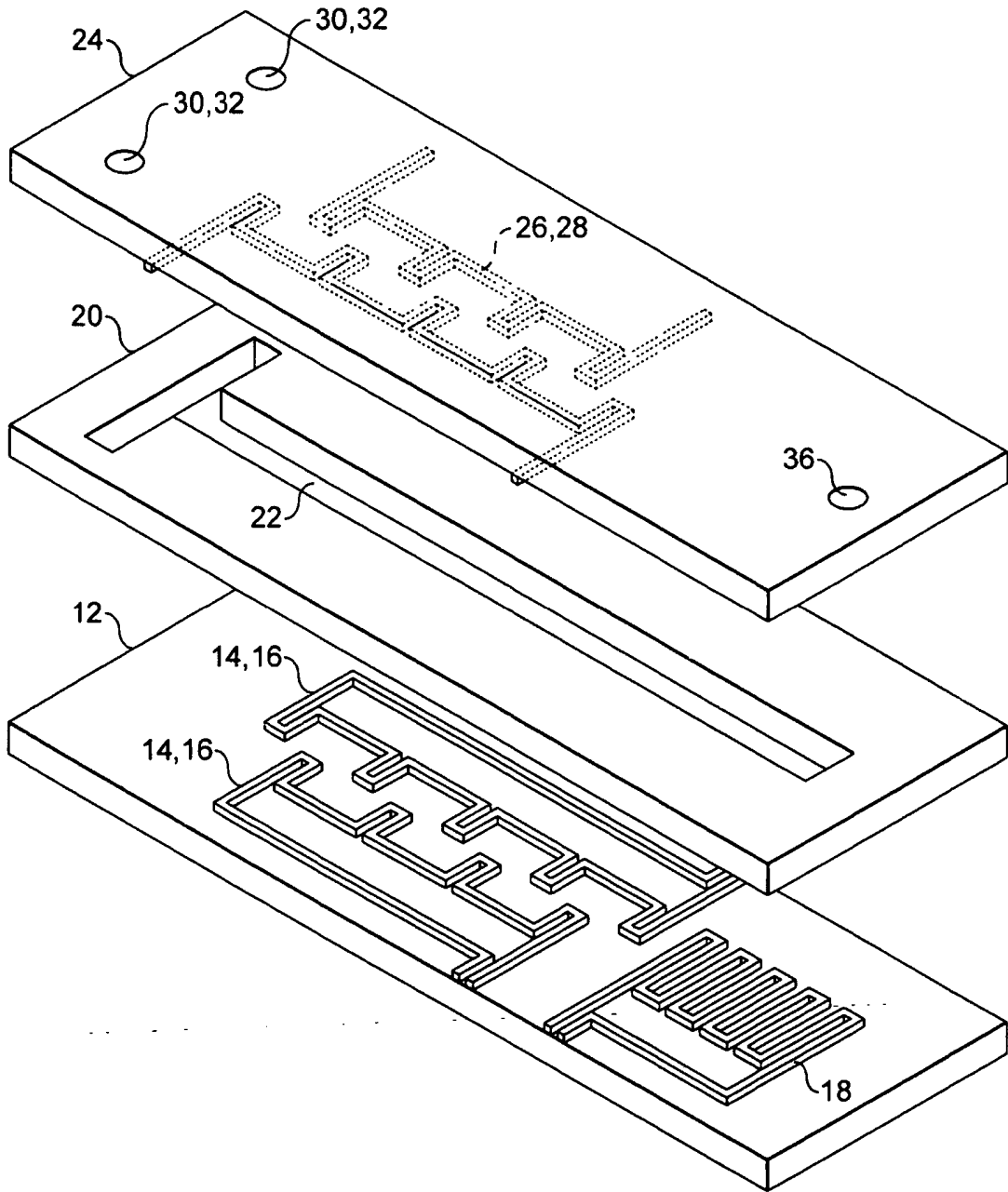


FIG. 1

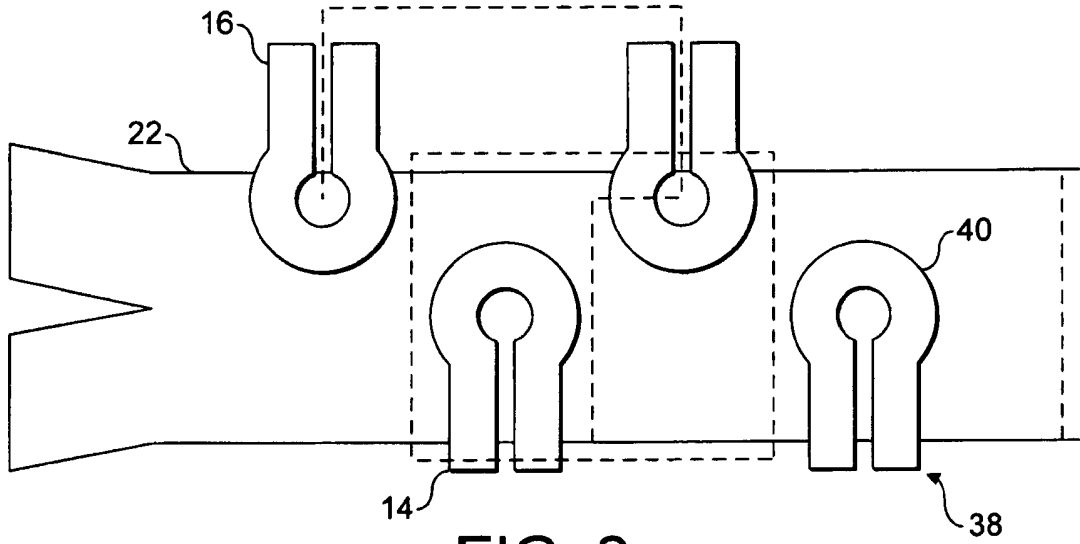


FIG. 2

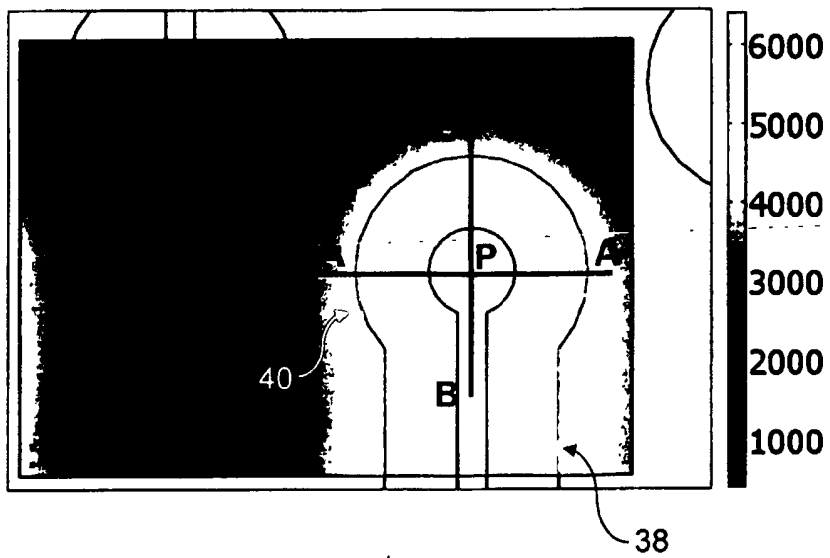
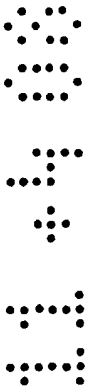


FIG. 3



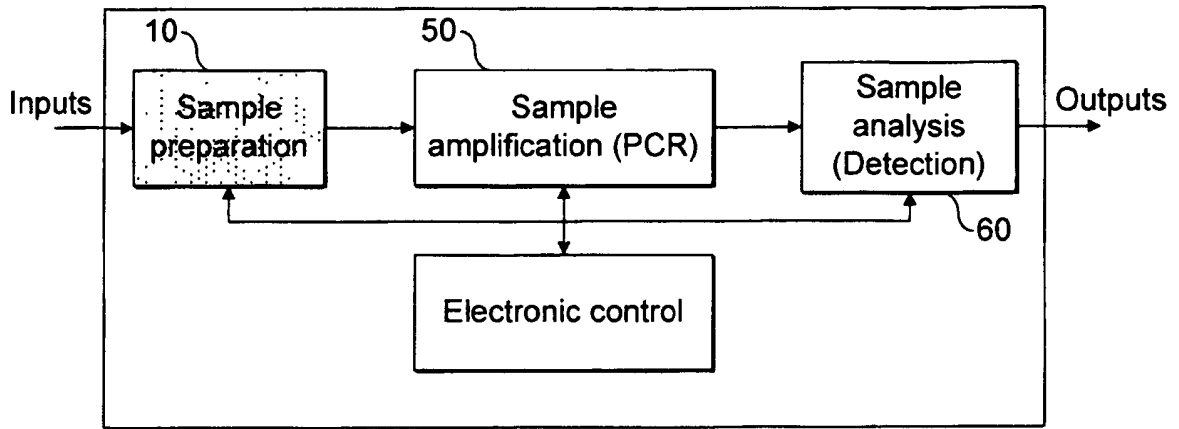


FIG. 4a

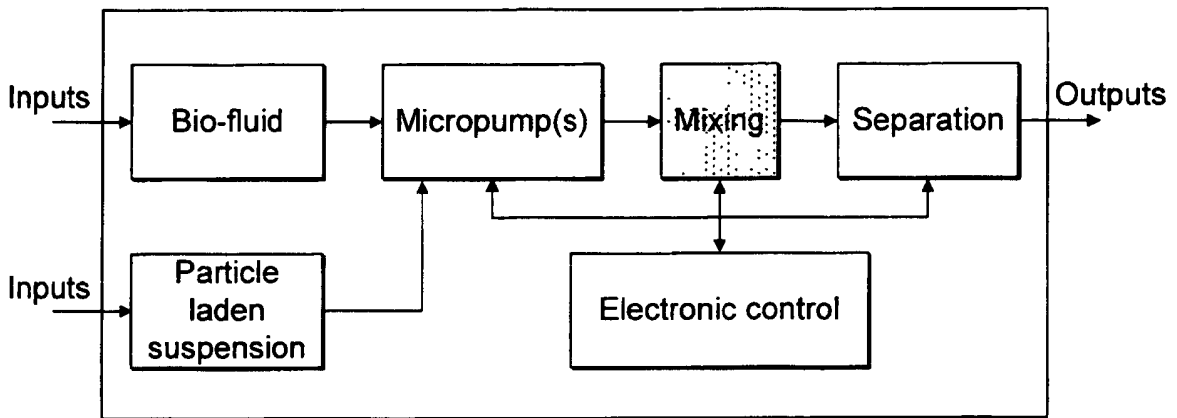


FIG. 4b

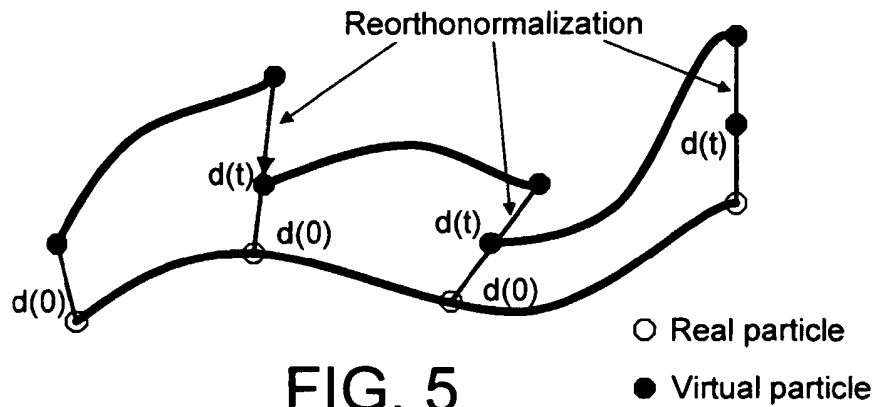


FIG. 5

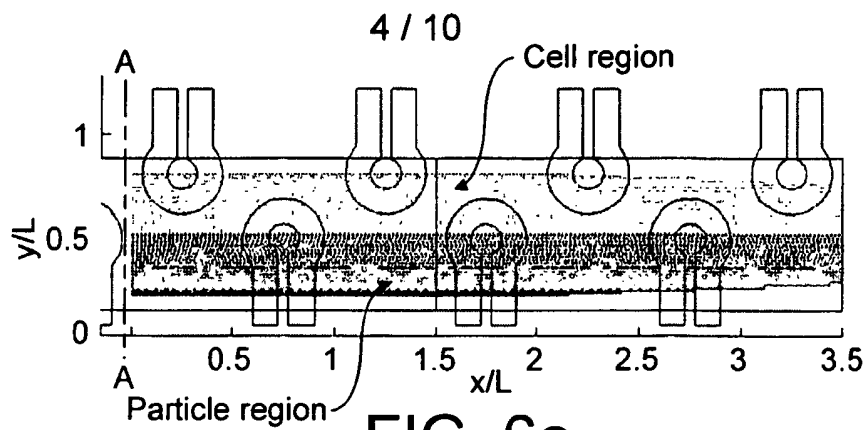


FIG. 6a

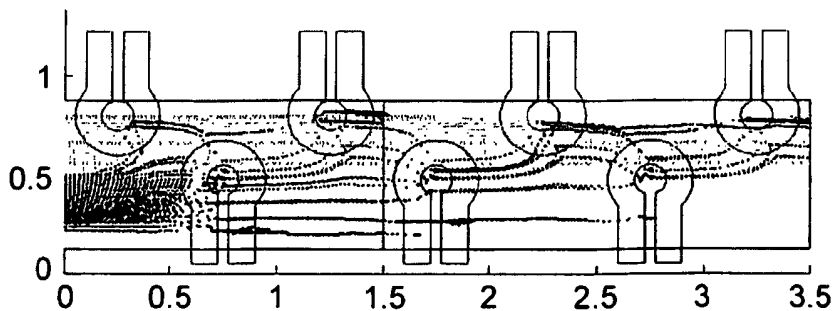
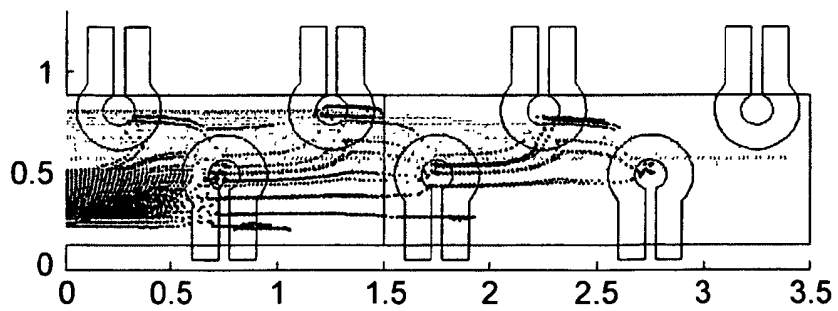
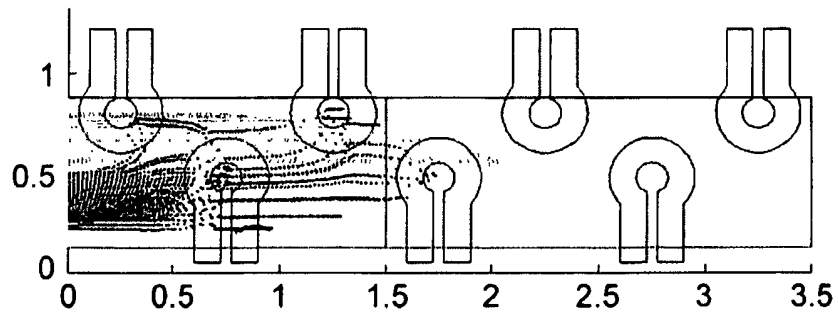
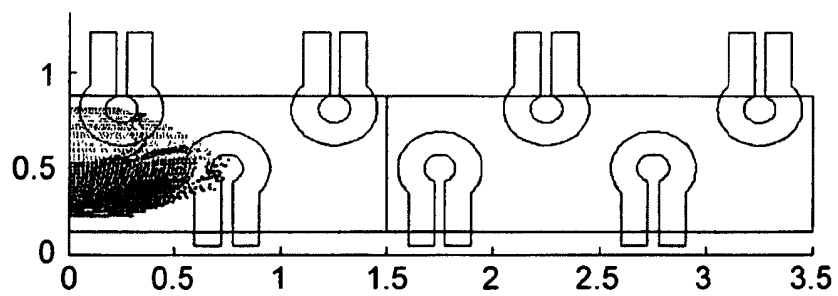


FIG. 6b



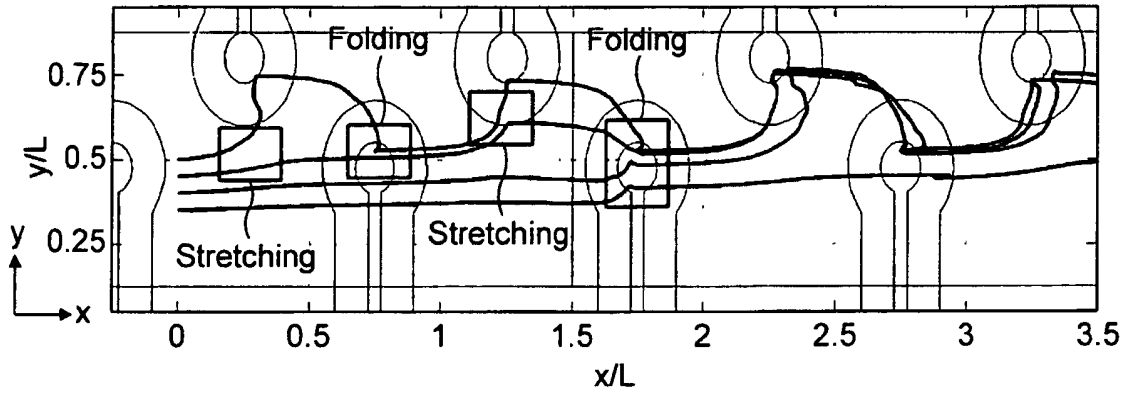


FIG. 7

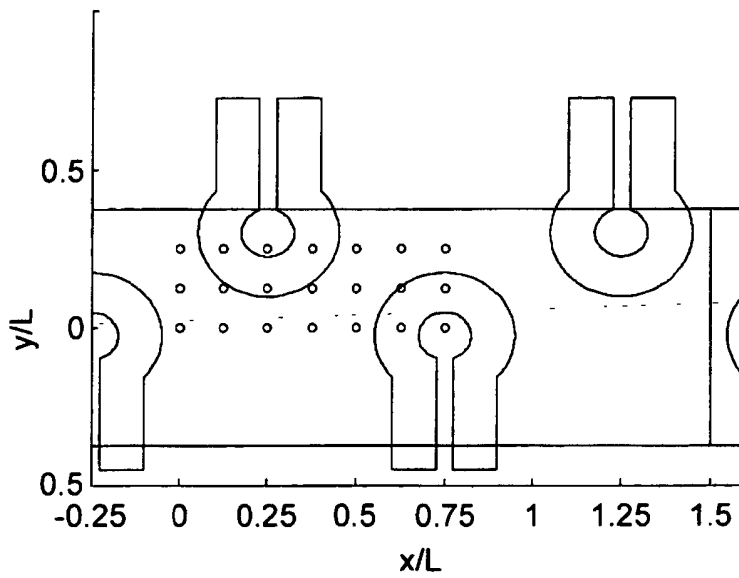
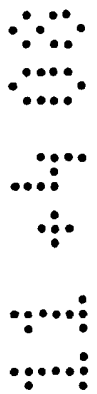


FIG. 8



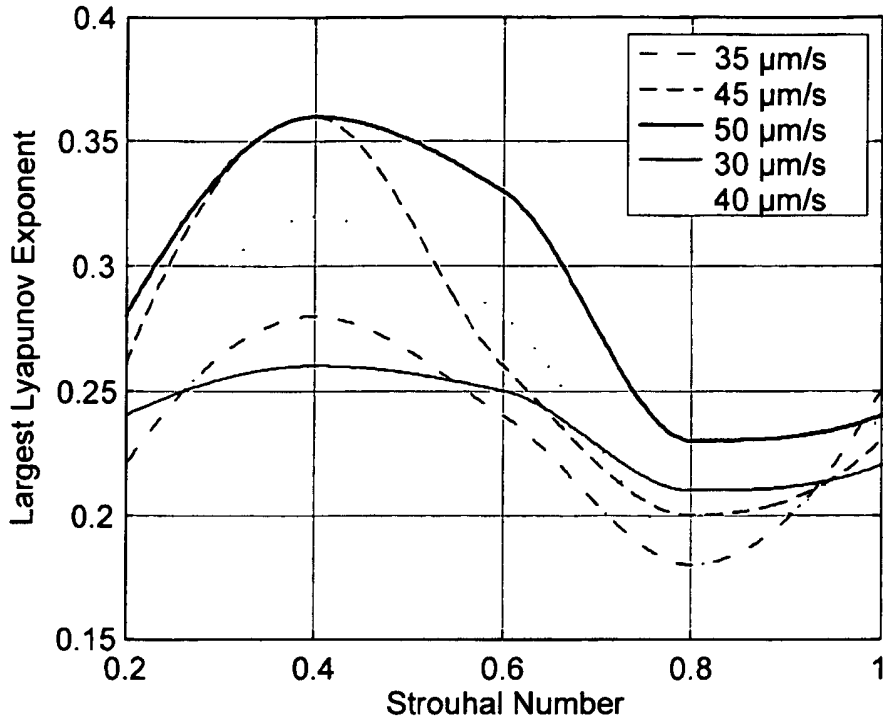


FIG. 9

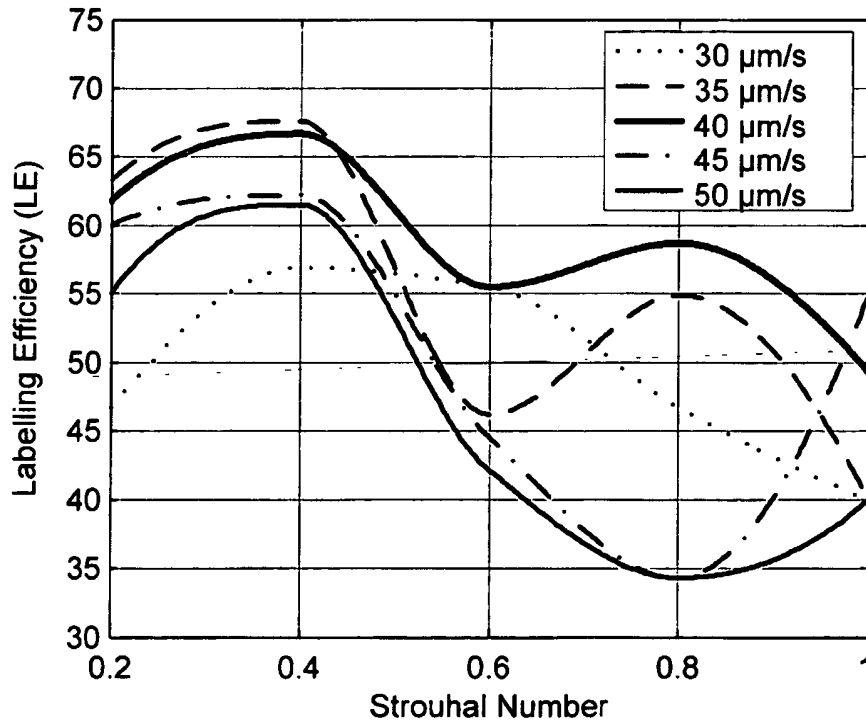


FIG. 10



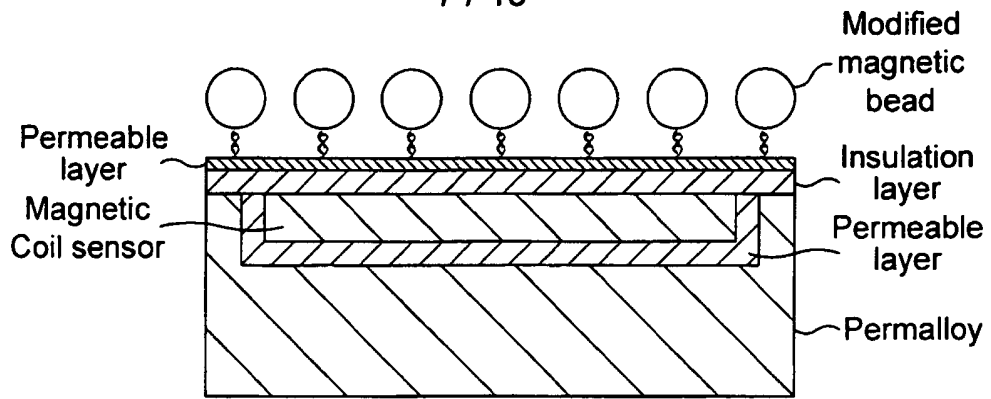


FIG. 11

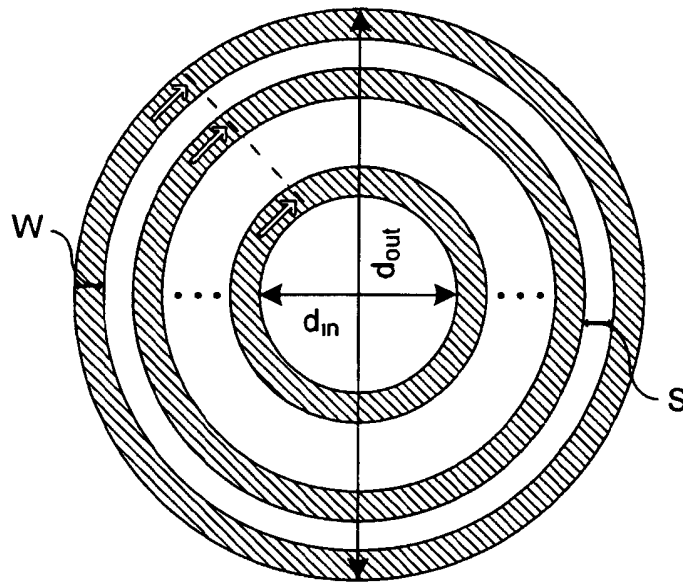


FIG. 12a

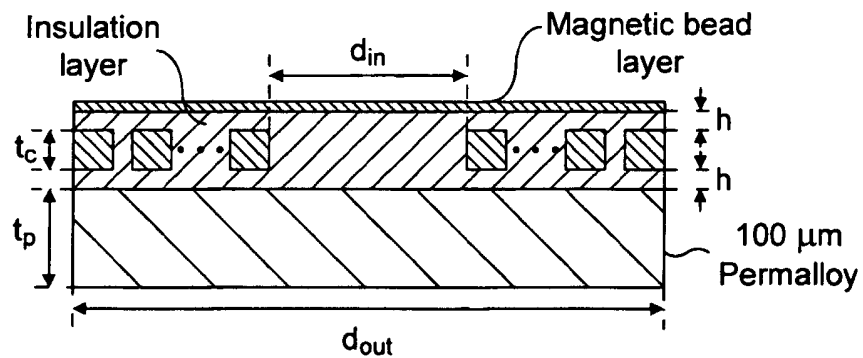


FIG. 12b



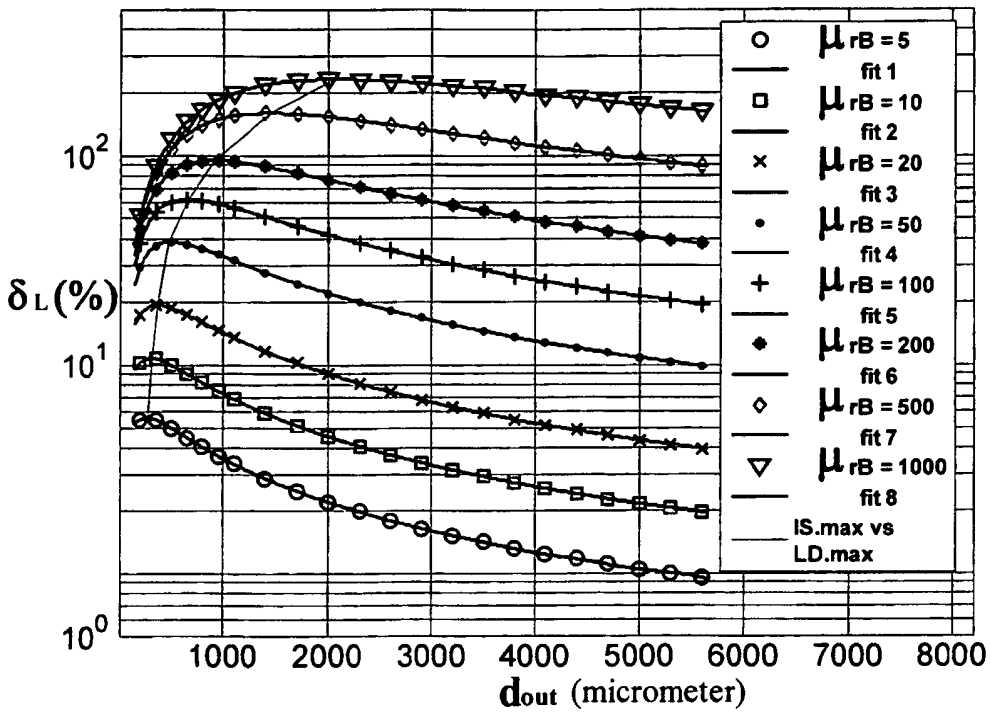


FIG. 14

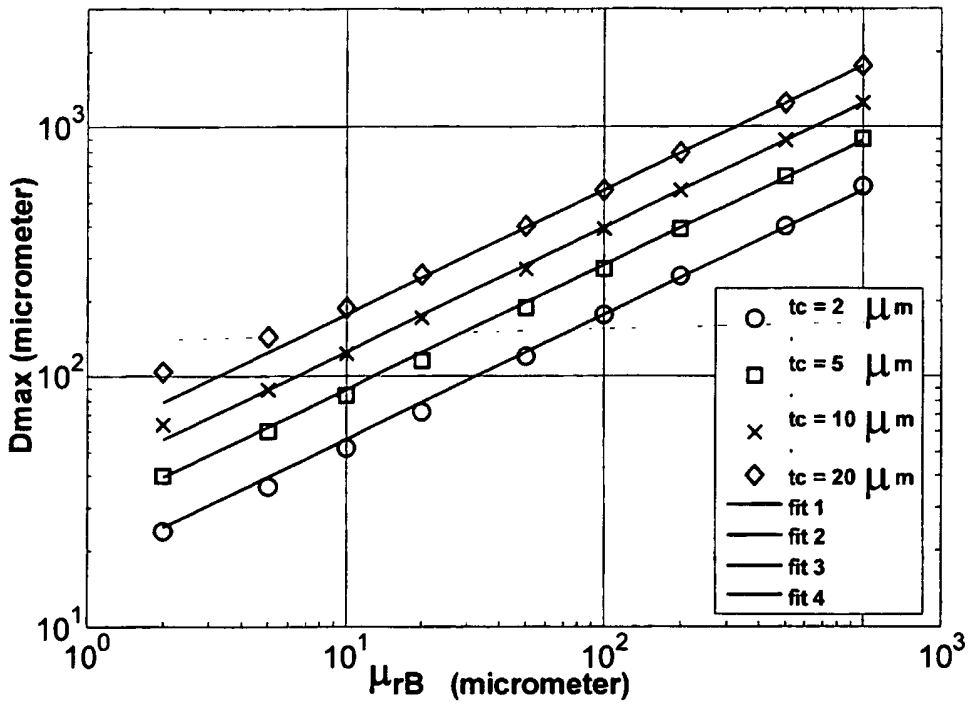
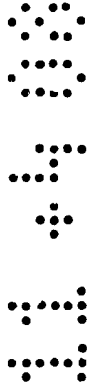


FIG. 15a



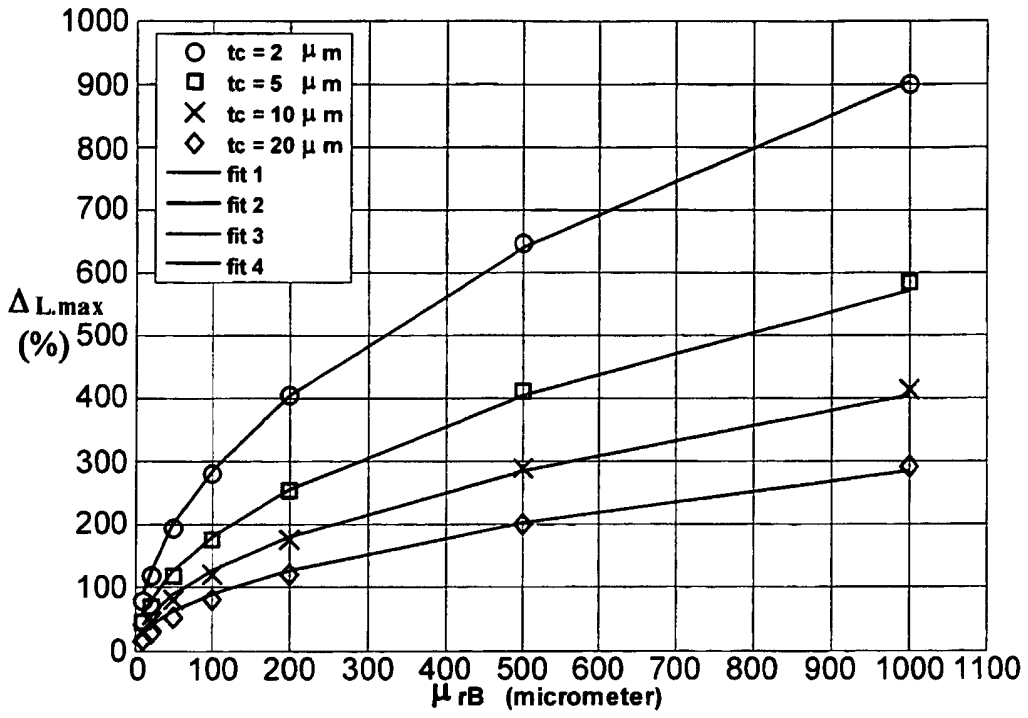


FIG. 15b

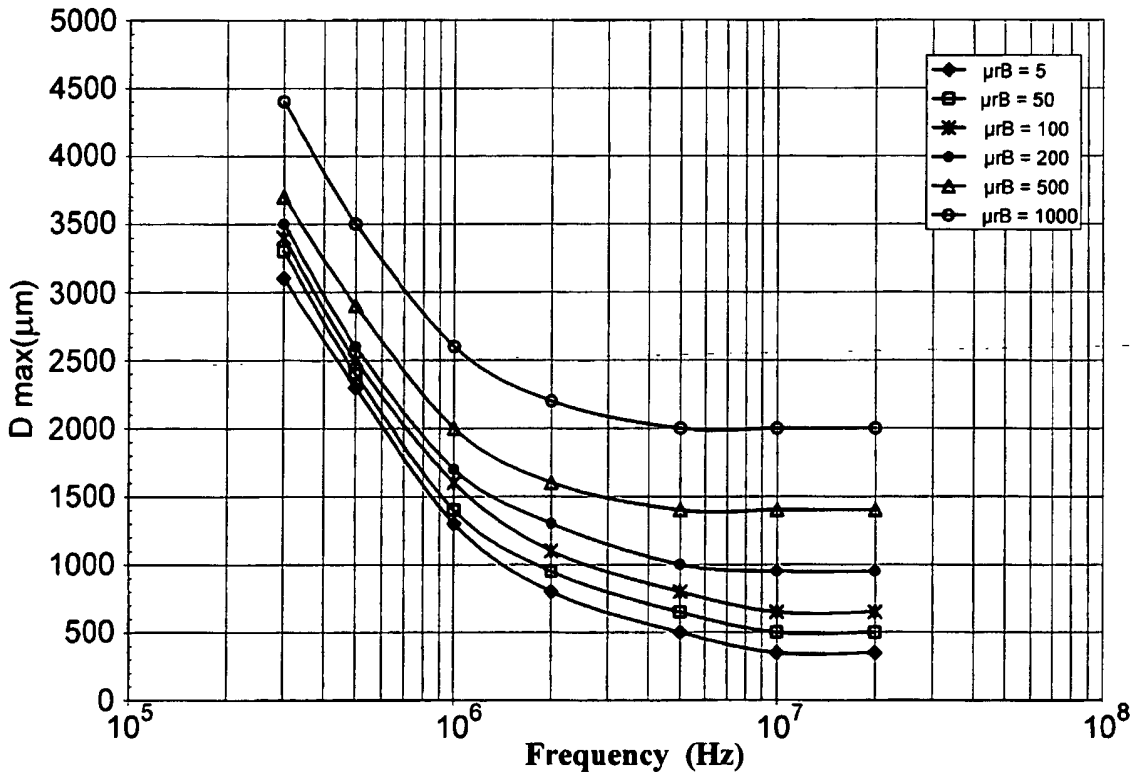


FIG. 16a

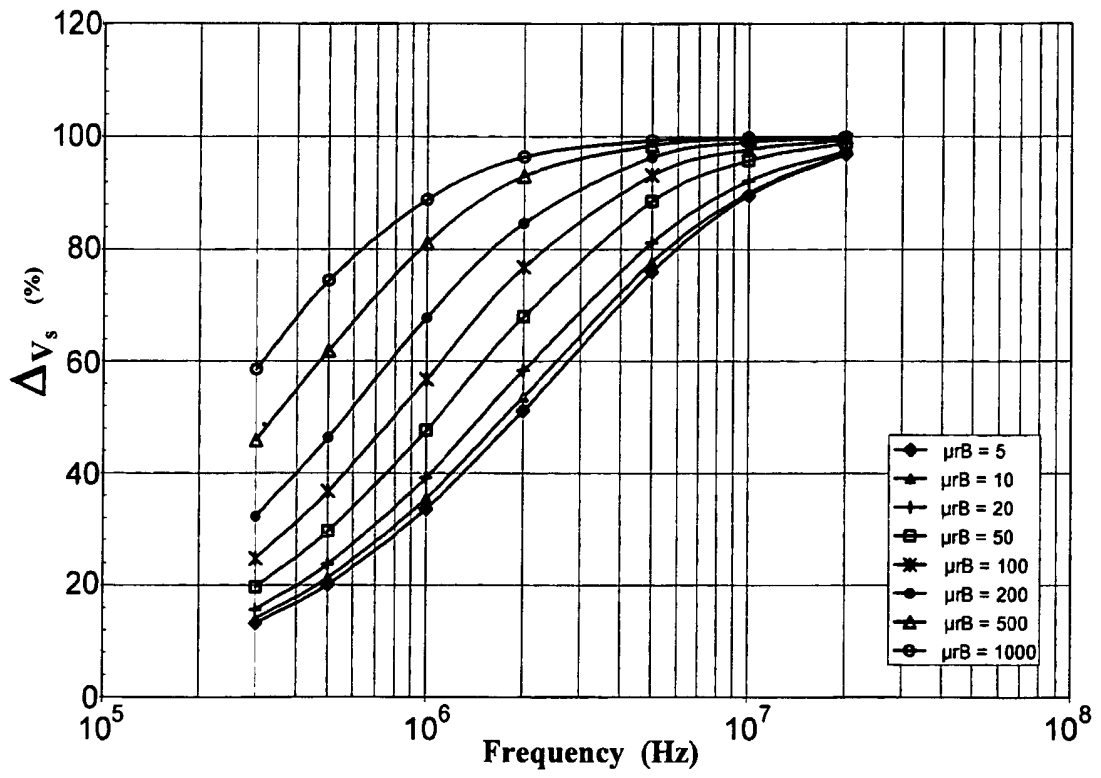


FIG. 16b

Microfluidic Device

Summary

5

The current invention relates to a microfluidic device and to methods of its use for isolating and detecting an analyte from a biological sample.

10 Introduction

Over the past decade, the advent of Micro-Electro-Mechanical Systems (MEMS) which is based on the miniaturization of mechanical components and their integration with micro-
15 electrical systems, has created the potential to fabricate various structures and devices on the order of micrometers. This technology takes advantage of almost the same fabrication techniques, equipment and materials that were developed by semi-conductor industries. The range of MEMS
20 applications is growing significantly and is mainly in the area of micro-sensors and micro-actuators. In recent years, miniaturization and integration of bio-chemical analysis systems to MEMS devices has been of great interest which has led to invention of Micro Total Analysis Systems (μ -TAS) or
25 Lab-on-a-Chip (LOC) systems.

The main advantages of μ -TAS over traditional devices lie in lower fabrication costs, improvement of analytical performance regarding quality and operation time, small
30 size, disposability, precise detection, minimal human interference and lower power consumption. Moreover, the problem of rare chemical and samples which restrain the

application of genetic typing and other molecular analyses has been resolved by employment of μ -TAS.

5 However, whilst there has been a great deal of work in core areas, for example, miniaturizing PCR for expedited amplification of DNA in the microchip format, less effort has been exerted towards miniaturizing DNA purification methods. In fact, most of the currently demonstrated microfluidic or microarray devices pursue single
10 functionality and use purified DNA or homogeneous sample as an input sample. On the other hand, practical applications in clinical and environmental analysis require processing of samples as complex and heterogeneous as whole blood or contaminated environmental fluids. Due to the complexity of
15 the sample preparation, most available biochip systems still perform this initial step off-chip using traditional bench-top methods. As a result, rapid developments in back-end detection platforms have shifted the bottleneck, impeding further progress in rapid analysis devices, to front-end
20 sample preparation where the "real" samples are used. A problem with the currently known microfluidic devices is performing efficient chaotic mixing in these platforms, this usually needs existence of moving parts, obstacles, grooves, and twisted or three dimensional serpentine channels. The
25 structures of these components tend to be complex, however, requiring complicated fabrication processes such as multi-layer stacking or multi-step photolithography.

Suzuki, H., et al (J. microelectromechanical systems, 2004,
30 vol 13, no.5 779-790) disclose a magnetic force driven chaotic mixer in which physical obstacles in the microchannel are used in conjunction with microconductors

embedded in the base of the channel, which act to manipulate magnetic beads back and forth, to facilitate mixing of the sample and the beads.

5 EP 1462174 A1 discloses a device for controlled transport of magnetic beads between a position X and a position Y, wherein the beads are transported by applying successively a series of local magnetic fields generated by triangular current carrying structures in which the current density is
10 non constant, resulting in the beads accumulating at the tips of the current carrying structures in the region having the highest charge density.

WO 2006004558 discloses a biochip for sorting and lysing
15 biological samples which makes use of dielectrophoretic forces to retain and recover desired cells from a sample.

It is an object of the current invention to provide a microfluidic device which provides improved mixing of
20 liquids in a microchannel, and also provides simpler fabrication and which overcomes or mitigates the problems of the prior art particularly coagulation of whole blood samples.

25 Summary of the Invention

According to the present invention there is provided a microfluidic device comprising;

30 i) an inlet;

ii) a first layer comprising at least first and second current carrying structures, wherein the at least first and second current carrying structures each comprise a plurality of teeth, and wherein the teeth of the first and second current carrying structures are offset such that the teeth of the first current carrying structure are positioned between the teeth of the second current carrying structure;

iii) a second layer comprising a first microfluidic chamber in fluid communication with the inlet and positioned above the at least first and second current carrying structures of the first layer; and

iv) a third layer comprising at least third and fourth current carrying structures wherein the at least third and fourth current carrying structures each comprise a plurality of teeth, and wherein the teeth of the third and fourth current carrying structures are offset such that the teeth of the third current carrying structure are positioned between the teeth of the fourth current carrying structure;

and wherein the at least third and fourth current carrying structures are positioned in the third layer so as to be above the first microfluidic chamber and such that the teeth of the third current carrying structure are positioned substantially vertically above or offset from the teeth of the first current carrying structure and the teeth of the fourth current carrying structure are positioned substantially vertically above, or offset from the teeth of the second current carrying structure;

characterised in that the teeth have a stem having substantially elliptical tip.

It will be understood that the term elliptical refers to a tip having an ovoid or circular conformation. In a preferred embodiment, the tip is circular.

It will further be understood that the elliptical configuration of the teeth of the device result in a magnetic field which is more evenly distributed about the tooth, as compared to other shapes of tooth, such as triangular, where the magnetic field is only stronger at the tip.

Preferably, the current carrying structures are embedded in the first and third layers. More preferably, the current carrying structures are between $0.1\mu\text{m}$ to $10\mu\text{m}$ below the surface of the first and third layers. Even more preferably, between $0.1\mu\text{m}$ and $5\mu\text{m}$. Most preferably, between $0.1\mu\text{m}$ and $2\mu\text{m}$.

It will be apparent to the skilled person that the device may also include a permalloy layer located within or adjacent the first and/or third layers distal to the microchannel to increase the magnetic field generated by the device.

In a preferred embodiment, the first microfluidic chamber is a substantially straight channel. In a further preferred embodiment, the substantially straight channel has a region having increased dimensions forming a chamber proximal to the inlet.

It will be understood that when device is in use this region acts to increase the rate at which a sample liquid can be mixed. This is of particular use where the sample is a liquid which is liable to thicken or coagulate, for example whole blood. The use of blood as the sample is of particular interest in devices which are designed as home use or point of care use, because the sample can be easily obtained by a simple needle prick.

10

In a particularly preferred embodiment the inlet opens directly into the region having increased dimensions and the current carrying devices extend into this region such that chaotic mixing of the sample begins immediately the sample enters the device.

15

Preferably, the first and/or third layers further comprises a fifth current carrying structure. More preferably, the fifth current carrying structure is located so as to be distal to the inlet.

20

In a preferred embodiment the first microfluidic chamber forms a lysis and extraction unit. In one particularly preferred embodiment the device is useful for the analysis of whole blood.

25

Preferably, the microfluidic device further comprises a second microfluidic chamber in fluid communication with the first microfluidic chamber, wherein the second microfluidic chamber is an amplification chamber. More preferably, the amplification chamber is a PCR chamber.

30

It will be understood that the skilled person would be able to include the second chamber as such amplification chambers are well known in the art for example as described by Young, S. S., et al (J. Micromechanics and Microengineering, 2003
5 13; 768-774).

In a further embodiment, the microfluidic device comprises a third microfluidic chamber in fluid communication with the second microfluidic chamber, said third microfluidic chamber
10 comprising a sensor for detecting the presence of an analyte.

In a particularly preferred embodiment, the sensor comprises a mutual inductance device.
15

In a yet further preferred embodiment, the microfluidic device comprises at least one integrated pump for effecting movement of a fluid from chamber to chamber. Preferably, the integrated pumps are magnetic pumps.
20

Preferably, the microfluidic device further comprises means for applying a voltage to each of the current carrying structures independently in a predetermined order and for a predetermined period.
25

Preferably, the period is in the range of 1-10 seconds, more preferably, less than 5 seconds.

Preferably, the microfluidic device further comprises at
30 least a first fluid reservoir.

In one embodiment, the at least a first reservoir is in fluid communication with the first microfluidic chamber. Preferably, the at least first reservoir is integrated into the device.

5

In a further embodiment, the first microfluidic chamber forms the first fluid reservoir.

Preferably, the fluid comprises superparamagnetic beads.

10

More preferably, the fluid also comprises lysis buffer.

In a still further embodiment, the microfluidic device further comprising at least a second fluid reservoir.

15

It will be apparent that the fluid may comprise other constituents, for example, it may optionally comprise an anticoagulant.

20 According to a second aspect of the current invention, there is provided a lab-on-chip system for preparing a sample comprising a biological molecule, the system comprising;

a) the device according to the first aspect;

25

b) means for introducing the sample and the fluid into the first microfluidic chamber.

30 Preferably, the the first, second, third and fourth current carrying structures of the device have a voltage applied thereto in a predetermined sequence.

In a preferred embodiment, a fifth current carrying structure acts to retain the superparamagnetic particles in the first microfluidic chamber.

5 It will be understood that the superparamagnetic particles may have any suitable diameter, preferably they have an average diameter from 50nm to 3 μ m.

Preferably, the superparamagnetic particles are
10 functionalised so as to bind to an analyte of interest. More preferably, the analyte is a nucleic acid.

In a preferred embodiment the system further comprises a second reservoir containing a wash buffer in fluid
15 communication with the first microfluidic chamber. Even more preferably, the system further comprises a third reservoir containing an elution buffer in fluid communication with the first microfluidic chamber.

20 It will be understood that the sample may be any suitable biological material. Preferably the sample comprises at least one cell. More preferably, the sample comprises a whole blood sample.

25 In a preferred embodiment, the fluid further comprises a lysis buffer.

In an even more preferred embodiment, the fluid further comprises an anticoagulant.

30

According to a third aspect of the current invention there is provided a method for the isolation of an analyte

comprising a biological molecule from a sample, said method comprising the steps of:-

- 5 i) introducing the sample into the inlet of the device according to the first aspect:
ii) introducing a fluid comprising superparamagnetic particles into the first microfluidic chamber of the device;
iii) applying a voltage to the first, second, third and fourth current carrying structures of the device in a
10 predetermined sequential order so as to cause electric currents to pass therethrough;

wherein, step i) can be performed prior to, concomitantly with or subsequently to step ii); and wherein, said
15 superparamagnetic particles are functionalised so as to bind to the analyte of interest;

and wherein step iii) is performed concomitantly with or immediately after step i);
20

characterised in that said electric current causes the current carrying structures to become non-permanently magnetised resulting in magnetic actuation of said superparamagnetic particles in 3 dimensions within the
25 microfluidic chamber, said magnetic actuation of said superparamagnetic particles resulting in chaotic mixing of said sample and said fluid resulting in an increased chance of the functionalised superparamagnetic particles coming in to contact with the analyte.

30

As mentioned above, the elliptical configuration of the teeth of the device result in a magnetic field which is more

evenly distributed about the tooth, as opposed to other shapes of tooth, such as triangular, where the magnetic field is stronger only at the tip. This results in greater mixing due to chaotic movement of the beads.

5

In a preferred embodiment the device further comprises a fifth current carrying structure, the fifth current carrying structure having a voltage applied thereto subsequently to step iii) wherein the superparamagnetic particles are
10 attracted to and retained on the fifth current carrying structure through magnetic interactions.

Preferably, the current passing through each current carrying structure is in the range of 100mA to 1A. More
15 preferably, 100mA to 750mA. Most preferably, less than 500mA

In a preferred embodiment, the method comprises the further step of introducing a wash solution into the first microfluidic chamber of the device, preferably, once the
20 superparamagnetic particles have been retained on the fifth current carrying structure.

The method optionally comprises the further step of introducing an elution solution into the first microfluidic
25 chamber of the device.

In a preferred embodiment, the voltage is applied to each of the first, second, third and fourth current carrying devices for sufficiently long so as to allow the beads to move to a
30 predetermined location in the first microfluidic chamber.

In one embodiment of the method of the third aspect the current carrying structures have the voltage applied in the order one, four, three, two. However, it will be apparent to the skilled person that the voltage can be supplied to the current carrying structures in any desired order so as to obtain optimum mixing of the fluid comprising the superparamagnetic particles and the sample.

In a preferred embodiment of the current invention the sample comprises at least one cell. More preferably, the sample is a blood sample.

Preferably, when the sample comprises at least one cell, the fluid further comprises lysis buffer and mixing of the sample with the buffer causes the cell to lyse.

Preferably, the analyte is a nucleic acid. More preferably, DNA.

The method of the third aspect preferably comprises the further step of detecting the presence of the analyte.

Preferably the velocity of flow of the sample through the first microfluidic chamber is in the range 20 - 100 $\mu\text{m/s}$.

According to a fourth aspect of the current invention there is provided a device for detecting the presence of an analyte in a sample, comprising;

- i) a spiral mutual inductor
- ii) an insulating layer having a first surface adjacent the spiral mutual inductor and an opposed second surface,

ii) a sample contacting layer having a first surface having at least one probe immobilised thereon and a second surface opposed to the first surface and positioned so as to be adjacent the second surface of the insulating layer,

5

wherein the spiral mutual inductor comprises a first coil and a second coil.

In one preferred embodiment of the fourth aspect the first and second coils are positioned such that the first coil is positioned vertically above the second coil.

10

In a second preferred embodiment, the first and second coils are interwound.

15

It will be understood by the skilled person that the presence of the analyte is detected by passing an alternating current through the first coil and monitoring the second coil for changes in induced voltage.

20

Preferably, the probe is a nucleic acid. More preferably, the probe is DNA.

In a preferred embodiment the device further comprises a permalloy layer located adjacent the spiral mutual inductor distal to the insulating layer.

25

Preferably, the insulating layer comprises silicon dioxide

It will be understood that the immobilisation layer may comprise any suitable material, for example, gold, agarose

30

or Si_3N_4 . Preferably, the immobilisation layer comprises an agarose gel.

According to a fifth aspect of the current invention,
5 thereis provided a method of detecting an analyte in a liquid sample, comprising the steps of;

- 10 a) bringing the sample containing the analyte into contact with magnetic beads functionalised so as to bind the analyte,
- b) isolating the paramagnetic beads from the sample
- c) bringing the beads into contact with the device of the fourth aspect, wherein the at least one probe immobilised on the sample contacting layer binds to the analyte so as to
15 retain the paramagnetic beads at the surface;
- d) measuring the variation in the inductance of the spiral mutual inductor,

wherein, an increase in the mutual inductance indicates the
20 presence of the analyte in the sample.

Preferably, the analyte is a nucleic acid.

More preferably, the probe is a nucleic acid.
25

The invention will now be described in greater detail with reference to the following figures, in which:-

Figure 1, is an exploded view of a microfluidic device
30 according to the first aspect.

Figure 2, shows a diagrammatic representation of the configuration of the current carrying structures forming one mixing unit in one layer of the device.

5 Figure 3, shows one tooth of a current carrying structure showing the variation in magnetic field intensity.

Figure 4a, shows a diagrammatic representation of a lab-on-chip device comprising the microfluidic device according to
10 the first aspect

Figure 4b, shows a diagrammatic representation of an embodiment of the device according to the first aspect.

15 Figure 5 shows a representation of Sprott's method for calculating the Lyapunov component.

Figures 6a and 6b, show advection of cells within three and a half mixing units, a) without perturbation of cells and b)
20 with magnetic perturbation.

Figure 7, shows simulated chaotic advection of four particles.

25 Figure 8, shows the initial positions of individual particles for calculating the Lyapunov Exponent.

Figure 9, shows the variation of largest LE against driving parameters

Figure 10, shows the variation of labelling efficiency against driving parameters

Figure 11, shows a diagrammatic representation of the detector device according to the current invention showing hybridised DNA tagged with magnetic beads.

Figure 12, shows a diagrammatic representation of the sensor model used in design simulations a) top view of coil, b) lateral cross section.

Figure 13, shows an electrical model of the sensor.

Figure 14, shows the percentage change in coil inductance against outer coil diameter for different bead permeabilities.

Figure 15a, is a graph showing the optimal outer coil diameter at which output signal is maximised against bead permeability for different conductor thickness values.

Figure 15b, is a graph showing the corresponding maximised inductance percentage change for the inductors of Fig 15a.

Figure 16a, is a graph showing the optimal outer coil diameter at which output signal is maximised against bead permeability for different frequencies.

Figure 16b is a graph showing the corresponding maximised sensor voltage for the frequencies of Fig 16a

Detailed Description

The micromixer 10, as shown in Fig. 1 comprises a base layer 12 formed from glass having three serpentine conductors 14, 16, 18 embedded therein. A central layer 20 formed from PDMS comprising a straight channel 22 which is located above the serpentine conductors 14, 16, 18 and a upper layer 24 fomred from glass having two further serpentine conductors 26, 28 embedded therein, two inlet ports 30, 32 and an outlet port 36.

10

An example of the dimensions of the device are shown in Fig. 2 where a top-view of one mixing unit with its boundaries is illustrated. Each mixing unit comprises two adjacent teeth from each conductor . Channel 22 is 150 μ m wide and 50 μ m deep. Conductors 14, 16 are in the shape of teeth 38 having circular tips 40 and are 35 μ m high and 35 μ m wide in the section and distances between centres of circular tips 40 of the conductors are 100 μ m and 65 μ m in x and y directions, respectively. Each row of upper and lower conductors 14, 16 is connected to the power supply alternately. The mixing operation cycle consists of two phases. In the first half-cycle, one of the conductor arrays in switched on while the other one is off. In the next half-cycle, the status of conductor arrays is reversed. Each mixing unit consists of two adjacent teeth 38 from opposite conductor arrays and the mixer is composed of a series of such mixing units which are connected together. In 3-D configuration, the switching between conductors will occur every 0.25 of a cycle.

30 Fig. 3 shows one tooth 38 with the magnetic field generated near the circular tip 40 of the conductor when a current of

750 mA is injected into one conductor array and is turned off in the opposite array during a half cycle of activation. The greyscale map represents variations in the magnetic field intensity at 10 μm above the surface of the conductor where the maximum magnitude of the field is about 6000 A/m at the centre of the circular tip (point P). The maximum force (5.5 pN) is applied on particles near the conductor and inside the circle of its tip where the intensity of magnetic field is at its maximum value. Although the magnetic field is maximum at the centre point P, the force on particles is relatively small at this point. This is due to the fact that the magnetic force is proportional to the gradient of the field which is almost constant in the neighbourhood of the point P. In moving away from the conductor, the force drops significantly due to a dramatic decrease in the magnetic field which in turn affects the magnetic moment.

The microfluidic device as shown in Figs 1 and 2 may be integrated into "lab-on-chip" devices such as those shown diagrammatically in Figs 4a and b. In Fig 4a, the device comprises a sample preparation device 10, as shown in Fig 1, linked in series to an amplification chamber 50 and a sample analysis unit 60 comprising a detector.

25

Figure 4b, shows the sample preparation device 10 in greater detail. The device comprises an inlet to a micropump, linked to a mixing region and a separation region distal to the inlet.

Use of the lab-on-chip device as shown in figure 4 for the isolation and preparation of a DNA sample involves four steps including:

- cell lysis
- 5 ▪ DNA binding
- washing to purify/separate contaminants
- resuspension

The first two steps are performed in the chaotic mixer
10 followed by downstream processes in separator. Firstly,
human blood and particle laden lysis buffer are introduced
to the microchannel through two inlet ports using external
pumps or integrated micropumps. Mixing of the particles is
performed by applying local and time-dependent magnetic
15 field generated by micro-conductors to produce chaotic
advection in the motion of the particles through
magnetophoretic forces. The embedded high aspect-ratio
conductors allow a relatively large current to generate
strong magnetic fields to move magnetic particles.
20 Conductors on both top and bottom glass wafers are required
to perform an efficient spatial mixing. Using a proper
concentration of particles in lysis buffer, chaotic
advection of the particles can be transferred to the fluids
pattern, therefore, mixing the lysis buffer and blood.
25 During the mixing and cell lysis, released DNA molecules are
adsorbed onto the particles' surface.

After the mixing, the whole solution is then flowed
downstream and the intact DNA/particles are separated from
30 other contaminants by using another serpentine conductor
fabricated at the bottom of the channel. This conductor is
activated by a constant DC current and due to the generated

magnetic field; particles are gathered at the bottom surface of the channel while other contaminants are washed out with flow. Subsequently, washing buffer is introduced into the channel, which washes and removes remaining contaminants.

5 Finally, conductors are switched off and resuspension buffer is pumped into the system and the purified DNA/particles are resuspended in it. The sample can now be used directly for PCR as the DNA is released upon heating the DNA/particle complex above 65°C as required by a standard PCR protocol.

10

Chaotic microfluidic mixer design

Functionalized nano and microparticlees or beads offer a large specific surface for chemical binding and may be

15 advantageously used as a "mobile substrate" for bioassays and in vivo applications (Gijs 2004). Due to the presence of magnetite (Fe_3O_4) or its oxidized form maghemite ($\gamma\text{-Fe}_2\text{O}_3$), magnetic particles are magnetized in an external magnetic field. Such external field, generated by a

20 permanent magnet or an electromagnet, may be used to manipulate these particles through magnetophoretic forces and therefore result in migration of particles in liquids.

By virtue of their small size; ranging from 100 μm down to 5 nm (Pankhurst et al. 2003), particles lose their magnetic

25 properties when the external magnetic field is removed, exhibiting superparamagnetic characteristics. This additional advantage has been exploited for separation of desired biological entities, e.g., cell, DNA, RNA and protein, out of their native environment for subsequent

30 analysis, where particles are used as a label for actuation. Prior to separation of the bio-cell/particle complex from contaminants, magnetic particles should be distributed

throughout the bio-fluidic solution which contains target cells. This is done by a mixing process which helps to tag the target with particles. In the next stage, only those cell attached to magnetic particles will be isolated in the
5 separation process, while the rest of the bio-fluidic mixture remains unaffected by the magnetic force. Separation of particles in microdevices based on magnetophoretic forces has been reported in the literature (Choi et al. 2001; Do et al. 2004; Ramadan et al. 2006).

10

Nevertheless, in micro-scale devices where the Reynolds number is often less than 1, mixing is not a trivial task due to the absence of turbulence. In such circumstances, mixing relies merely on molecular diffusion. Diffusion
15 coefficient for a dilute solution of relatively large spheres in small, spherical molecules is estimated by Stokes-Einstein equation as follows (Mitchell 2004):

$$D = \frac{\kappa_B T}{3\pi\mu d} \quad (1)$$

20 where K_B is Boltzmann's constant, T is the absolute temperature, μ is the dynamic viscosity of the solvent, and d is the diameter of diffusing particle. The diffusion time constant τ is proportional to the diffusion distance squared ($\tau=L^2/D$) which can be up to the order of 10^5 seconds for
25 particules with 1 μm diameter dispersed in water solution diffusing a distance of 100 μm . Obviously, such a diffusion time is not realistic and some improving mechanisms need to be employed to facilitate the mixing process.

30 In order to enhance the diffusion process, (multi-) lamination with different types of feed arrangements has

been used in passive micromixers (Koch et al. 1999). The idea is to reduce the diffusion length scale using narrow mixing channels. Split-and-recombine (SAR) configurations (Haverkamp et al. 1999) can also enhance mixing through
5 splitting and later joining the streams. Such configurations create consecutive multi-laminating patterns and increase the interfacial area. However, one disadvantage of using lamination for mixing of the particle laden fluids is the high probability of clogging in narrow channels. Another
10 approach is to generate chaotic advection either by fabrication of special geometries and structures (e.g., obstacles (Wang et al. 2002), 3D channels (Liu et al. 2000), and grooves (Stroock et al. 2002)) or by applying external forces (e.g., dielectrophoretic (Deval et al. 2002),
15 electroosmotic (Lin et al. 2004), pressure (Deshmukh et al. 2000) and thermal (Tsai et al. 2002) fields) in passive and active devices, respectively. Chaotic advection increases interfacial area and, consequently, enhances the mixing process. Recently, in addition to separation,
20 magnetophoretic forces are exploited to enhance the mixing of the particles in solution (Rida et al. 2003); Rong et al. 2003; Suzuki et al. 2004). Here we describe the design of a chaotic magnetic particle-based micromixer and a numerical model in order to characterize the device with different
25 driving parameters. To this end, a combination of electromagnetic, microfluidic and particle dynamics models has been used.

Conductors are utilized to produce magnetophoretic
30 (hereafter, magnetic) forces and, therefore, chaotic pattern in the motion of particles and intensify the labelling of bio-cells. Two flows; target cells suspension and particle

laden buffer, are introduced into the channel and manipulated by pressure-driven flow (see Fig. 2). While the cells follow the mainstream in upper half section of the channel (transported by convection of the suspending bio-
5 fluid), the motion of magnetic particles is affected by both surrounding flow field and localized time-dependent magnetic field generated by periodical activation of two serpentine conductor arrays. Particles from various positions in the upstream and downstream sides are attracted towards the
10 centre of the nearest activated tip where the maximum magnetic field exists. Chaotic patterns are produced in the motion of particles through utilizing a proper structural geometry and periodical current injection in conductors, thereby enhancing the spread of particles in the channel.

15

The magnetic force on particles is a function of the external magnetic field gradient and the magnetization of the particle. In de-ionized water, the magnetic force exerted on the particle in the linear area is described by:

20

$$r_p = \int V_p \cdot dt = \int (V_f + \frac{F_m}{3\pi\mu d}) \cdot dt$$

where: d is the diameter of the spherical particle

H is the external magnetic field

F_m is magnetic force

25 μ_r is relative permeability of the particle

μ_0 is permeability of the vacuum

Magnetic force is applied along the gradient of the external field and the particles are attracted towards higher
30 magnetic field regions. Relative permeability and diameter of the reference particle used in this study (M-280, Dynabeads, Dynal, Oslo, Norway) are 2.83 μm and 1.76, respectively.

It should be noted that the magnetic force is three-dimensional and the z-component of the force is downward, which together with gravity, pull the particles towards the bottom of the channel and restrict their motion to a two-dimensional pattern. In fact, this component has no contribution to the chaotic motion of the particles and is assumed not to be influential on the process of mixing. Therefore, in this study planar forces close to the surface of the channel's bottom are of interest and simulation procedure is conducted on a two-dimensional basis.

Motion of the particles relative to the media can be assumed as a creeping flow and therefore, drag force on the particles can be evaluated by Stokes' law. The velocity of the particle due to the magnetic and drag forces can be described by Newton's second law:

$$m_p \frac{\partial V}{\partial t} = F_m - 3\pi\mu dV \quad , \quad V_m = \frac{F_m}{3\pi\mu d} \quad (2)$$

where m_p is the particle mass, V is the relative velocity of the particle with respect to the fluid, μ is the dynamic viscosity and d is the diameter of the particle. Term V_m is terminal velocity, which is reached by the particles after the exertion of the magnetic force. Particle relaxation time ($\tau = d^2\rho/18\mu$) for the used particle (density of 1.4 g/cm³) and viscosity of water at room temperature (0.001 kg/ms), is in the order of 0.1 μ s. Therefore, acceleration phase in the motion is negligible and particle is assumed to react to the magnetic forces with no delay. Total velocity of the particle at each moment (V_p) would be the sum of the

velocity due to fluid field (V_f) and the velocity due to magnetic field (V_m).

A two-dimensional numerical simulation is carried out
5 assuming that there are no magnetic or hydrodynamic
interactions between particles (one-way coupling) and motion
of the particles is treated as if they are moving
individually. This assumption is valid for small particles
at low concentration in suspension, namely less than 10^{15}
10 particles/ m^3 (C. Mikkelsen and H. Bruus, "Microfluidic
capturing-dynamics of paramagnetic bead suspensions," Lab
Chip, vol. 5, pp.1293-7, 2005) Newtonian fluid (water)
field and time-dependent magnetic field are computed using
commercial multiphysics finite element package Comsol
15 (COMSOL, UK) and velocities of the particles due to these
fields are extracted. Then trajectories of the particles are
evaluated by integrating the sum of velocities using Euler
integration method in Matlab:

$$r_p = \int V_p \cdot dt = \int (V_f + \frac{F_m}{3\pi\mu d}) \cdot dt \quad (3)$$

20 Trajectories of the cells are obtained using the same
Lagrangian tracking method with this exception that cells
are magnetically inactive. Likely optimized structural
geometry and dimensions (as mentioned earlier) and also a
permissible current magnitude at which heat generation is
25 not an issue (750 mA), obtained from preliminary studies are
considered as constant parameters and two driving
parameters; frequency of magnetic activation and flow
velocity, are varied. Ratio of frequency to velocity is
proportional to the dimensionless Strouhal Number (St):

$$St = \frac{fL}{V} \quad (4)$$

where f is the frequency, L is the characteristic length (here, distance between two adjacent teeth), and V is the mean velocity of the fluid. Simulations are conducted for the range of $St=0.2-1$. The size of biological entities may vary from a few nano-meters (proteins) to several micrometers (cells). In this study, cells are considered to be spheres of 1 μm diameter. The bulk velocity of flow is in the order of 10 $\mu\text{m/s}$, which yields a Reynolds number of the order of 10^{-3} , indicating that the flow is laminar.

In order to quantitatively evaluate the degree of mixing and efficiency of the system, two criteria are computed for the investigated range of simulation parameters. Efficiency of labelling of the target cells was used as the main index for characterizing the mixer. This method uses the idea of monitoring the trajectories of the particles and cells to predict their collision (if any) in the mixing domain (H. Suzuki, et al, "A chaotic mixer for magnetic bead-based micro cell sorter," J. Microelectromech. Syst., vol. 13, pp. 779-90, 2004). It is assumed that collision happens when the distance between the centre of the spherical particle and cell becomes smaller than the sum of their radii, then cell is attached to the particle. Attachment of multiple cells to a single particle is possible and after each collision the trajectories of the particles must be recalculated using new free-body force diagram. Although the driving force is the same for the cell/particle complex (magnetic force is applied merely on the particles), the drag coefficients need to be modified according to the number of the attached

cells. Subsequently, Labelling Efficiency (LE), i.e., ratio of the tagged cells to the total number of entered cells, is calculated over a specific period of mixing process.

5 Supplement to the stated index, largest Lyapunov exponent (λ) was used to quantify the chaotic advection of magnetic particles as a common definition of the mixing quality. Here Sprott's method (J. C. Sprott, Chaos and Time-Series Analysis, Oxford University Press, Oxford, 2003) is used to
10 calculate the largest Lyapunov exponent (hereafter λ_1). This method utilizes the general idea of tracking two initially close particles, and calculates average logarithmic rate of separation of the particles. The numerical procedure is shown in Fig. 5. For any arbitrary particle, a virtual
15 particle is considered with a minute distance of $d(0)$ from the chosen particle and trajectories of these particles are tracked. At the end of each time-step, the new distance, $d(t)$, between real and virtual particles and also the value of $\ln|d(t)/d(0)|$ are calculated. The virtual particle is then
20 placed at distance $d(0)$ along its connecting line to the real particle. After repeating this process for several time-steps, λ_1 will be converged and is evaluated by:

$$\lambda_1 = \lim_{n \rightarrow \infty} \frac{1}{n\Delta t} \sum_{i=1}^n \ln \frac{|d_i(t)|}{|d(0)|} \quad (5)$$

where Δt is the duration of one time-step and n is the
25 number of steps. Examination of λ_1 for various particles reveals that generally after a period of 20s, λ_1 approaches its converged value. Therefore, both indices of LE and λ_1 are calculated for a period of 20s of mixing.

Fig. 6a illustrates the position of the particles and cells while advecting within three and half mixing units. Bio-cells (red dots) and magnetic particles (blue dots) enter the first mixing unit (across line A-A) from the left in upper and lower halves of the section, respectively, and with the same concentration. When there is no magnetic actuation, both cells and particles remain in their initial section and simply follow the streamlines of the parabolic velocity profile in Poiseuille flow. In this situation, tagging might occur only in the central region of the channel along the interface between two halves. All dimensions are normalized to the characteristic length.

Fig. 6b illustrates a typical effect of the magnetic actuation ($St=0.4$, $V=40 \mu\text{m/s}$) within the same mixing units at different snapshots. When the external field is applied, particles travel across the streamlines as well as the interface. Therefore, they find the opportunity to spread in upper section where they can meet and tag the cells. Magnetically inactive cells will have the same behaviour as previous situation when no perturbation was applied. As it can be observed, some particles far from the central line of the channel remain in the lower section as the magnetic forces in these regions are not strong enough to attract them during the lower array activated half-cycle.

25

In order to explain the basis for chaotic advection in the proposed micromixer, trajectories of four particles as shown in Fig. 7 are considered as typical trajectories in the mixer. Particles are released in the first mixing unit uniformly with the spacing of $10 \mu\text{m}$ when $St=0.2$ and $V=45 \mu\text{m/s}$. During the first half cycle, first array (conductor

30

I) is on and second array (conductor II) is off. Particle I feels a strong magnetic force in y direction and tends to move in this direction while it is advected by the mainstream in x direction. Note that depending on its
5 location in the channel which determines both drag force in the Poiseuille flow and magnetic force, particle I can have a positive or negative velocity in x direction. Particle 2 is farther from the conductor I and does not find any chance to be attracted upwards completely during the first half
10 cycle. Therefore, two initially nearby particles diverge inducing the mechanism of stretching which is marked with a rectangle. In this phase particle I is exposed to the target cells across different streamlines and captures them in case on any collision.

15

In the following half cycle, electric current is injected into the conductor II and turned off in conductor I. In this phase, particle 1 is free to move from the previous location and is further advected by the mainstream until it
20 approaches a region of strong enough magnetic force and, consequently, is pulled towards the centre of conductor II. Particle 2 is subject to a small magnitude of magnetic force in y direction but tends to move faster than the mainstream by virtue of magnetic force in x direction. In this phase,
25 particle 2 approaches and tags the target cells, if any, along one streamline. Folding is achieved where two distant trajectories converge and even in some operating conditions cross each other. Consecutive stretching and folding can be produced in this way which is the basis of chaos.

30

Particles 3 and 4 which are too far from the conductor I to be attracted, are dragged downstream by the fluid and

gradually move towards the upper half of the channel. After passing a few mixing units, almost all particles penetrate to cells' region and fluctuate in a chaotic regime confined to the tips of two conductors.

5

For computation of the largest Lyapunov exponent, 21 particles are uniformly distributed in upper half of the first mixing unit as the initial positions and λ_1 is calculated for each individual particle (see Fig. 8). The time period is 20s when the particles approach their constant value of λ_1 . In order to quantify the extent of chaos over the entire domain in the upper section (where cells exist), the average of λ_1 s of 21 particles is taken. Fig. 9 illustrates variation of LE for different driving parameters ($St=0.2-1$) where each graph represents the values of LE for a constant fluid velocity ($V=30-50 \mu\text{m/s}$). Results for λ_1 calculated over the same range of driving parameters are shown in Fig.10. The global variations of λ_1 is almost identical for different bulk flow velocities; the maximum chaos happens at $St=0.4$, while the minimum occurs at $St=0.8$. LE exhibits a similar behaviour at Strouhal numbers less than 0.6 which means that an increase in chaos leads to an increase in labelled cells.

25 Maximum values for λ_1 and LE are realized at $St=0.4$, which are 0.36 and 67%, respectively. At higher Strouhal numbers (namely 0.8), two indices show different variations.

Although at high bulk flow velocities (larger than $40 \mu\text{m/s}$) a good agreement between two indices can still be observed, in the case of lower velocities they show contradicting behaviours. At low flow velocities, some particles are

30

advected until they are attracted to the centre of one tip in the upper conductor array. In the vicinity of the channel wall, flow velocity is much less than the central region of the channel. Since the magnetic forces are significantly large in the centre of the conductor, these particles will be stuck in this areas. Even after the current is switched to the opposite array, due to the low fluid velocity, particles will not have the opportunity to escape from the previous conductor. Therefore, in the next period, particles are dragged towards the same region hastily and again become trapped. In such operating conditions, the mixer is only partially chaotic, and the mixing is incomplete. However, trapped particles act like fixed posts, which may tag multiple cells, thereby increasing the value of LE. Although the efficiency is relatively high, in practice it is a challenging issue where trapped particles can clog the channel. However, when the Strouhal number is low, i.e., in case of longer time periods, particles have the chance to move away from these centres, even though the velocity is low.

A two-dimensional numerical study is performed in order to characterize the efficiency of the micromixer. Maximum labelling efficiency is found to be 67%. Lyapunov exponent as an index of the chaotic advection is found to be highly dependent on the Strouhal number where the maximum chaotic strength is realized in Strouhal numbers close to 0.4. It is shown that labelling efficiency in the mixer cannot be used as a stand alone index. Therefore, both indices need to be taken into account while characterizing the device.

Inductance sensor design

Traditionally, DNA hybridization detection is performed by using fluorescent tagging and optical read-out techniques. 5 These techniques are efficient in conventional biology labs where specific protocols are followed by skilled technicians using expensive equipment. Moreover, conventional detection of DNA is a time consuming procedure which adds an extra cost to the whole process. To overcome these problems, 10 considerable effort has been made for more than a decade to miniaturize and integrate the whole processes in a single disposable chip. Although detection of DNA by optical methods is reliable and well practised, it cannot be easily implemented on electronic chips. Alternative methods with 15 potential for miniaturization have been investigated in recent years. Among these methods are electrochemical techniques (R. M. Umek et al., "Electronic detection of nucleic acids, a versatile platform for molecular diagnostics," *J. Molecular Diagnostics*, vol. 3, pp. 74-84, 20 2001), piezoelectric sensors (T. Tatsuma, et al, "Multichannel quartz crystal microbalance," *Anal. Chem.*, vol. 71, no. 17, pp. 3632-3636, Sep. 1999), impedance based techniques (F. Patolsky, et al, "Highly sensitive amplified electronic detection of DNA by biocatalyzed precipitation of 25 an insoluble product onto electrodes," *Chemistry - A European Journal*, vol. 9, pp. 1137-1145, 2003), and capacitance techniques (E. Souteyrand, et al, "Direct detection of the hybridization of synthetic homo-oligomer DNA sequences by field effect," *J. Phys. Chem. B*, vol. 101, 30 pp. 2980-2985, 1997). Micron-sized magnetic beads have also been widely used as labels in DNA detection (J. Fritz, et

al, "Electronic detection of DNA by its intrinsic molecular charge," *Proc. Nat. Acad. Sci.*, vol. 99, no. 22, pp. 14 142-6, 2002) (L,Moreno-Hagelsieb, et al, "Sensitive DNA electrical detection based on interdigitated Al/Al₂O₃ microelectrodes," *Sens. Actuators B, Chem.*, vol. 98, pp. 5 269-274, 2004) (P. A. Besse, et al, "Detection of a single magnetic microbead using a miniaturized silicon Hall sensor," *Appl. Phys. Lett.*, vol. 80, pp. 4199-4201, 2002). Using magnetic beads allows easy manipulation of DNA and 10 therefore may also facilitate mixing and separation protocols (D. R. Baselt, et al "A biosensor based on agnetoresistance technology," *Biosens. Bioelectron.*, vol. 13, no. 7-8, pp. 731-739, Oct. 1998) (J. C. Rife, et al "Design and performance of GMR sensors for the detection of 15 magnetic microbeads in biosensors," *Sens. Actuators A, Phys.*, vol. 107, no. 3, pp. 209-218, 2003).

This example relates to a DNA hybridization detection sensor that uses magnetic beads attached to DNA strands as 20 detectable particles. Increased concentration of magnetic beads due to DNA hybridization is detected in the form of inductance variations. The response of a planar spiral coil sensor to different types of magnetic beads is investigated and the effects of coil geometry as well as frequency on the 25 performance of the sensor are numerically evaluated.

The sensor 100 of the current invention for DNA hybridization detection is illustrated in Fig. 11. The sensor 100 comprises a core 102 which is a planar spiral 30 inductor which is sandwiched between an insulating layer 104 on the top and a layer of permalloy 106 in the bottom. The insulating layer 104 is covered with a permeable layer 108

to which probe DNAs 110 can attach and be immobilized. This layer could be any of standard surface treatments on gold coating or $\text{SiO}_2\text{-Si}_3\text{N}_4$. Magnetic beads functionalized with target DNAs 112 are applied to this surface. Specific
5 Hybridization of target and probe DNA will result in formation of a layer of magnetic beads 112 above this surface 108. This layer is of high magnetic permeability and acts as one half of the magnetic core for the inductor. The underlying permalloy layer 106 acts as the other half of the
10 magnetic core and completes the magnetic circuit. Formation of this magnetic circuit allows the magnetic flux to pass through easily and leads to an increase in the coil inductance. This property is used for detection of hybridization process.

15

Parameters affecting the Inductance

The inductance of the spiral coil is a function of various geometrical as well as physical parameters. The important
20 geometrical parameters as depicted in Fig. 12 are defined as follows:

d_{out} : Coil outer diameter

d_{in} : Coil inner diameter

t_c : Conductor thickness

t_p : Thickness of permalloy layer

The effect of interwinding distance S and the conductors thickness w are expressed in terms of fill factor (FF). The
25 relative permeability of magnetic beads, μ_{rB} and the thickness of the bead layer t_h , formed after hybridization, are the physical parameters affecting the coil inductance.

Electrical Model of the Sensor

The electrical model of the sensor is shown in Fig. 13. The coil is driven by an AC current source and the coil voltage is measured as the sensor output. After formation of the bead layer, the coil inductance is increased and the sensor output, V_s , will be changed. This amplitude of this voltage is used in order to detect the hybridization.

The amplitude of V_s can be expressed as follows:

$$V_s = \sqrt{R_c^2 + (\omega L_c)^2} I, \quad (1)$$

10

The voltage V_s is measured and its normalized variation is calculated to indicate the presence of the bead layer due to occurrence of hybridization. The frequency of the current source may be chosen in a range where R_c is constant. This means that for a particular sensor and source frequency, the voltage V_s is merely dependent on the inductance L_c and hence, the normalized variations of V_s may be calculated as follows:

15

20

$$\delta_{V_s} = \frac{V_s(L_{c2}) - V_s(L_{c1})}{V_s(L_{c1})} \quad (2)$$

25

To understand the way δ_{V_s} varies with respect to different geometrical and physical parameters explained above, the variations in L_c is computed numerically. This is then used to determine how the coil voltage will change in terms of different parameter values.

30

Based on the described concept, a three dimensional model of the sensor was simulated using the finite element package COMSOL FEMLAB Multiphysics v.3.2. Details of the model used

in the simulation are shown in Fig. 12. The model was simulated for a layer of magnetic beads with effective thickness of $2\mu\text{m}$ and different relative permeabilities. The normalized variations of the coil inductance, described in Equation 3, is computed numerically before and after hybridization and the results are presented in Fig. 14.

$$\delta_L = \frac{L_c(d_{out}, t_c, \mu_{rB}, t_B, t_p) - L_c(d_{out}, t_c, \mu_{rB} = 1, t_B = 0, t_p)}{L_c(d_{out}, t_c, \mu_{rB} = 1, t_B = 0, t_p)} \quad (3)$$

The graphs of Fig. 14 show how δ_L changes with respect to the outer diameter d_{out} for different values of μ_{rB} . The values adopted for the other parameters are shown in Table 1.

Table 1: Various parameters and their corresponding values that are used in coupled inductors simulation.

Parameter	Explanation	Quantity
t_c	Thickness of Conductor	$20 \mu\text{m}$
w_c	Width of Conductor	$20 \mu\text{m}$
s	Space Between Conductors	$30 \mu\text{m}$
FF	Fill Factor (occupied area of conductors of the coil to the total coil area)	$\%80$
h	Gap between coil	$10 \mu\text{m}$

and bead layer
which is occupied
with insulator

As shown in Fig. 14, for each value of the relative permeability, the sensor output is maximum at a specific value of d_{out} which may be denoted as D_{max} . It should be noted that the value of D_{max} is increasing with respect to μ_{rB} as shown by the dashed curve in Fig. 14.

To minimize the effect of permalloy on the signal, a very thick layer of permalloy ($\mu_{rp} = 100\mu m$) has been used. Also a large space-domain (7mm x 14mm) has been adopted in order to minimize computational errors.

In order to design a sensor with maximum response, it is useful to have the optimal coil diameter D_{max} in terms of different bead permeabilities and conductor thickness. The graphs in the Fig. 15a show the results of simulation for D_{max} in terms of μ_{rB} and t_c . Once the optimal diameter of the coil and the conductor thickness is known, it is useful to evaluate the magnitude of the output signal. These information may be derived from the graphs of Fig. 15b which depict the maximum change $\Delta_{L,max} = \delta_{L_i}(at D_{max})$ corresponding to optimal values of D_{max} in terms of bead permeability and conductor thickness.

25

The Effect of Frequency on Sensor Output

To see the behaviour of the sensor output with respect to frequency, the quantity δ_{ν_i} is computed for different bead permeabilities. The parameter values are as in Table 1 and the simulation results are shown in Fig. 16. For each value
5 of the relative permeability and frequency, the sensor output is maximum at a specific value of d_{out} which is again denoted as D_{max} . The graphs of Fig. 16a show how these values are related to frequency. The corresponding sensor
10 output $\Delta_{\nu_i} = \delta_{\nu_i}(at D_{max})$ which are normalized by $\Delta_{L,max} = \lim_{\omega \rightarrow \infty} (\Delta_{\nu_i})$ are graphed in Fig. 16b.

References

R. M. Umek et al., "Electronic detection of nucleic acids, a versatile platform for molecular diagnostics," *J. Molecular*
5 *Diagnostics*, vol. 3, pp. 74-84, 2001.

T. Tatsuma, Y. Watanabe, N. Oyama, K. Kitakizaki, and M. Haba, "Multichannel quartz crystal microbalance," *Anal. Chem.*, vol. 71, no. 17, pp. 3632-3636, Sep. 1999.

10

F. Patolsky, A. Lichtenstein, I. Willner, "Highly sensitive amplified electronic detection of DNA by biocatalyzed precipitation of an insoluble product onto electrodes," *Chemistry - A European Journal*, vol. 9, pp. 1137-1145, 2003.

15

E. Souteyrand, J. P. Cloarec, J. R. Martin, C. Wilson, I. Lawrence, S. Mikkelsen, and M. F. Lawrence, "Direct detection of the hybridization of synthetic homo-oligomer DNA sequences by field effect," *J. Phys. Chem. B*, vol. 101, pp. 2980-2985, 1997.

20

J. Fritz, E. B. Cooper, S. Gaudet, P. K. Sorger, and S. R. Manalis, "Electronic detection of DNA by its intrinsic molecular charge," *Proc. Nat. Acad. Sci.*, vol. 99, no. 22, pp. 14 142-6, 2002.

25

L. Moreno-Hagelsieb, P. E. Lobert, R. Pampin, D. Bourgeois, J. Remacle, D. Flandre, "Sensitive DNA electrical detection based on interdigitated Al/Al₂O₃ microelectrodes," *Sens. Actuators B, Chem.*, vol. 98, pp. 269-274, 2004.

30

P. A. Besse, G. Boero, M. Demirre, V. Pott, and R. Popovic, "Detection of a single magnetic microbead using a miniaturized silicon Hall sensor," *Appl. Phys. Lett.*, vol. 80, pp. 4199-4201, 2002.

5

D. R. Baselt, G. U. Lee, M. Natesan, S. W. Metzger, P. E. Sheehan, and R. J. Colton, "A biosensor based on agnetoresistance technology," *Biosens. Bioelectron.*, vol. 13, no. 7-8, pp. 731-739, Oct. 1998.

10

J. C. Rife, M. M. Miller, P. E. Sheehan, C. R. Tamanaha, M. Tondra, and L. J. Whitman, "Design and performance of GMR sensors for the detection of magnetic microbeads in biosensors," *Sens. Actuators A, Phys.*, vol. 107, no. 3, pp. 209-218, 2003.

15

H. Suzuki, C. M. Ho, and N. Kasagi, "A chaotic mixer for magnetic bead-based micro cell sorter," *J. Microelectromech. Syst.*, vol. 13, pp. 779-790, 2004.

20

J. Do, J. W. Choi, and C. H. Ahn, "Low-cost magnetic interdigitated array on a plastic wafer," *IEEE Trans. Magnetics*, vol. 40, pp. 3009-3011, 2004.

25

J. W. Choi, T. M. Liakopoulos, and C. H. Ahn, "An on-chip magnetic bead separator using spiral electromagnets with semi-encapsulated permalloy," *Biosens. Bioelectron.*, vol. 16, pp. 409-16, 2001.

30

Q. Ramadan, V. Samper, D. Poenar, and C. Yu, "Magnetic-based microfluidic platform for biomolecular separation," *Biomed Microdevices*, vol. 8, pp. 151-8, 2006.

R. Rong, J. W. Choi, and C. H. Ahn, "A novel magnetic chaotic mixer for in-flow mixing of magnetic beads," in Proc. Of the 7th Int. Conf. on Miniaturized Chemical and Biochemical Analysts Systems, California, 2003, pp. 335-8.

T. B. Jones, Electromechanics of Particles, Cambridge University Press, Cambridge, 1995.

10 C. Mikkelsen and H. Bruus, "Microfluidic capturing-dynamics of paramagnetic bead suspensions," Lab Chip, vol. 5, pp.1293-7, 2005.

J. C. Sprott, Chaos and Time-Series Analysis, Oxford University Press, Oxford, 2003.

Claims

1. A microfluidic device comprising;

5

i) an inlet;

ii) a first layer comprising at least first and second current carrying structures, wherein the at least first and second current carrying structures each comprise a plurality of teeth, and wherein the teeth of the first and second current carrying structures are offset such that the teeth of the first current carrying structure are positioned between the teeth of the second current carrying structure;

10

15

iii) a second layer comprising a first microfluidic chamber in fluid communication with the inlet positioned above the at least first and second current carrying structures of the first layer; and

20

iv) a third layer comprising at least third and fourth current carrying structures wherein the at least third and fourth current carrying structures each comprise a plurality of teeth, and wherein the teeth of the third and fourth current carrying structures are offset such that the teeth of the third current carrying structure are positioned between the teeth of the fourth current carrying structure;

25

and wherein the at least third and fourth current carrying structures are positioned in the third layer so as to be above the first microfluidic chamber and such that the teeth of the third current carrying structure are positioned

30

substantially vertically above or offset from the teeth of the first current carrying structure and the teeth of the fourth current carrying structure are positioned substantially vertically above or offset from the teeth of the second current carrying structure;

characterised in that the teeth have a stem having substantially elliptical tip.

10 2. The microfluidic device according to claim 1, wherein the current carrying structures are embedded in the first and third layers.

3. The microfluidic device according to claim 2 wherein, 15 the current carrying structures are 0.1 μ m to 10 μ m below the surface of the first and third layers.

4. The microfluidic device according to any preceding claim, wherein the first microfluidic chamber is a 20 substantially straight channel.

5. The microfluidic device according to claim 4, wherein the substantially straight channel has a region having increased dimensions proximal to the inlet.

25

6. The microfluidic device according to claim 5, wherein the inlet opens directly into the region having increased dimensions.

30 7. The microfluidic device according to any preceding claim, wherein the first and/or third layers further comprises a fifth current carrying structure.

8. The microfluidic device according to claim 7, wherein the fifth current carrying structure is located so as to be distal to the inlet.

5

9. The microfluidic device according to any preceding claim, wherein the first microfluidic chamber forms a lysis and extraction unit.

10 10. The microfluidic device according to any preceding claim, further comprising a second microfluidic chamber in fluid communication with the first microfluidic chamber, wherein the second microfluidic chamber is an amplification chamber.

15

11. The microfluidic device according to claim 10, wherein the amplification chamber is a multiplexed PCR chamber.

12. The microfluidic device according to any preceding
20 claim, further comprising a third microfluidic chamber in fluid communication with the second microfluidic chamber, said third microfluidic chamber comprising a sensor for detecting the presence of an analyte.

25 13. The microfluidic device according to any preceding claim, further comprising at least one integrated micropump for effecting movement of a fluid from one chamber to second chamber.

30 14. The microfluidic device according to claim 13, wherein the integrated pumps are magnetic pumps.

15. The microfluidic device according to any preceding claim, further comprising means for applying a voltage to each of the current carrying structures independently in a predetermined order and for a predetermined period.

5

16. The microfluidic device according to any preceding claim, further comprising at least a first fluid reservoir.

17. The microfluidic device according to claim 16, wherein
10 the at least a first reservoir is in fluid communication with the first microfluidic chamber

18. The microfluidic device according to claim 16 or 17,
15 wherein the at least first reservoir is integrated into the device.

19. The microfluidic device according to claim 16, wherein the first microfluidic chamber forms the first fluid reservoir.

20

20. The microfluidic device according to any one of claims 16 to 19, wherein the fluid comprises superparamagnetic beads

25 21. The microfluidic device according to any one of claims 16 to 19, wherein the fluid comprises lysis buffer.

22. The microfluidic device according to any one of claims 16 to 21, further comprising at least a second fluid
30 reservoir.

23. The microfluidic device according to any one of claims 16 to 22, wherein the fluid optionally comprises an anticoagulant.

5 24. A lab-on-chip system for preparing a sample comprising a biological molecule, the system comprising;

a) the device of any one of claims 20 to 23;

10 b) means for introducing the sample and the fluid into the first microfluidic chamber.

25. The system according to claim 24, wherein in the first, second, third and fourth current carrying structures of the device have a voltage applied thereto in a predetermined sequence.

26. The system according to claim 24 or claim 25, wherein a fifth current carrying structure acts to retain the superparamagnetic particles in the first microfluidic chamber.

27. The system according to any one of claims 24 to 26, wherein the superparamagnetic particles have an average diameter from 50nm to 3 μ m.

28. The system according to any one of claims 24 to 27, wherein the superparamagnetic particles are functionalised so as to bind to an analyte of interest.

30

29. The system according to claim 28, wherein the analyte is a nucleic acid.

30. The system according to any one of claims 24 to 29,
further comprising a second reservoir containing a wash
buffer in fluid communication with the first microfluidic
5 chamber.

31. The system according to any one of claims 24 to 30,
further comprising a third reservoir containing an elution
buffer in fluid communication with the first microfluidic
10 chamber.

32. The system according to any one of claims 24 to 31,
wherein the sample comprises at least one cell.

15 33. The system according to any one of claims 24 to 32,
wherein the fluid further comprises a lysis buffer.

34. The system according to any one of claims 24 to 33,
wherein the fluid further comprises an anticoagulant.

20

35. A method for the isolation of an analyte comprising a
biological molecule from a sample, said method comprising
the steps of:-

- 25 i) introducing the sample into the inlet of the device of
any one of claims 1 to 23:
ii) introducing a fluid comprising superparamagnetic
particles into the first microfluidic chamber of the device;
iii) applying a voltage to the first, second, third and
30 fourth current carrying structures of the device in a
predetermined sequential order so as to cause electric
currents to pass therethrough;

wherein, step i) can be performed prior to, concomitantly
with or subsequently to step ii); and wherein, said
superparamagnetic particles are functionalised so as to bind
5 to the analyte of interest;

and wherein step iii) is performed concomitantly with or
immediately after step i);

10 characterised in that said electric current causes the
current carrying structures to become non-permanently
magnetised resulting in magnetic actuation of said
superparamagnetic particles in 3 dimensions within the
microfluidic chamber, said magnetic actuation of said
15 superparamagnetic particles resulting in chaotic mixing of
said sample and said fluid resulting in an increased chance
of the functionalised superparamagnetic particles coming in
to contact with the analyte.

20 36. The method according to claim 35, wherein the device
further comprises a fifth current carrying structure, the
fifth current carrying structure having a voltage applied
thereto subsequently to step iii) wherein the
superparamagnetic particles are attracted to and retained on
25 the fifth current carrying structure through magnetic
interactions.

37. The method according to claim 35 or 36, wherein the
microfluidic chamber is in the form of a substantially
30 straight channel.

38. The method according to any one of claims 35 to 37, wherein the current passing through each current carrying structure is in the range of 100mA to 1A.

5 39. The method according to claim 38, wherein the current passing through each current carrying structure less than 500mA

40. The method according to any one of claims 35 to 39,
10 comprising the further step of introducing a wash solution into the first microfluidic chamber of the device.

41. The method according to any one of claims 35 to 40,
15 comprising the further step of introducing a resuspension solution into the first microfluidic chamber of the device.

42. The method according to any one of claims 35 to 41,
comprising the further step of introducing an elution
solution into the first microfluidic chamber of the device.

20

43. The method according to any one of claims 35 to 42,
wherein the voltage is applied to each of the first, second,
third and fourth current carrying devices for sufficiently
long so as to allow the beads to move to a predetermined
25 location in the first microfluidic chamber.

44. The method according to any one of claims 35 to 43,
wherein the current carrying structures have the voltage
applied in the order one, four, three, two.

30

45 The method according to any one of claims 35 to 44
wherein the sample comprises a least one cell.

46. The method according to any one of claims 35 to 45,
wherein the fluid comprises lysis buffer.

5 47. The method according to claim 46 wherein, mixing of the
lysis buffer with the at least one cell causes the cell to
lyse.

48. The method according to any one of claims 35 to 47,
10 wherein the analyte is a nucleic acid.

49. The method according to any one of claims 35 to 48,
comprising the further step of detecting the presence of the
analyte.

15

50. The method according to any one of claims 35 to 49,
wherein the velocity of flow of the sample through the first
microfluidic chamber is 20 - 100 $\mu\text{m/s}$.

20 51. A device for detecting the presence of an analyte in a
sample, comprising;

i) a spiral mutual inductor

ii) an insulating layer having a first surface adjacent the
spiral mutual inductor and an opposed second surface,

25 iii) an immobilisation layer having a first surface having
at least one probe immobilised thereon and a second surface
opposed to the first surface and positioned so as to be
adjacent the second surface of the insulating layer,

30 wherein the spiral mutual inductor comprises a first coil
and a second coil.

52. The device according to claim 51, wherein the probe is a nucleic acid.

53. The device according to claim 52, wherein the probe is
5 DNA.

54. The device according to any one of claims 51 to 53, further comprising a permalloy layer located adjacent the spiral mutual inductor distal to the insulating layer.

10

55. The device according to any one of claims 51 to 54, wherein the insulating layer comprises silicon dioxide.

56. The device according to any one of claims 51 to 55,
15 wherein the sample contacting layer comprises an agarose gel.

57. A method of detecting an analyte in a liquid sample, comprising the steps of;

20

a) bringing the sample containing the analyte into contact with magnetic beads functionalised so as to bind the analyte,

b) isolating the magnetic beads from the sample

25 c) bringing the beads into contact with the device of any one of claims 51 to 56, wherein the at least one probe immobilised on the immobilisation layer binds to the analyte so as to retain the magnetic beads at the surface;

d) measuring the variation in the mutual inductance of the
30 spiral mutual inductor,

wherein, an increase in the mutual inductance indicates the presence of the analyte in the sample.

58. The method according to claim 57, wherein the analyte
5 is a nucleic acid.

59. The method according to claim 57 or 58, wherein the probe is a nucleic acid.

§3

Application No: GB0700653.9

Examiner: Mr Stuart Purdy

Claims searched: 1-50

Date of search: 9 May 2008

Patents Act 1977: Search Report under Section 17

Documents considered to be relevant:

Category	Relevant to claims	Identity of document and passage or figure of particular relevance
X	1-6, 9-25, 27-35, 37-50	US 2002/0036141 A1 (GASCOYNE) See whole document and note in particular figures 3A, 4C, and 8 and paras 73, 112, 114;
A	-	EP 1658890 A2 (SAMSUNG)
A	-	WO 03/057368 A1 (CAMBRIDGE UNIVERSITY)
A	-	EP 1462174 A1 (INTERUNIVERSITAIR MICROELEKTRONICA)
A	-	WO 2006/004558 A1 (AGENCY FOR SCIENCE, TECHNOLOGY & RESEARCH)

Categories:

X	Document indicating lack of novelty or inventive step	A	Document indicating technological background and/or state of the art.
Y	Document indicating lack of inventive step if combined with one or more other documents of same category	P	Document published on or after the declared priority date but before the filing date of this invention.
&	Member of the same patent family	E	Patent document published on or after, but with priority date earlier than, the filing date of this application

Field of Search:

Search of GB, EP, WO & US patent documents classified in the following areas of the UKC^X :

Worldwide search of patent documents classified in the following areas of the IPC

B01F; B01J; B01L; B03C; B81B; F04B; G01N

The following online and other databases have been used in the preparation of this search report

WPI & EPODOC

International Classification:

Subclass	Subgroup	Valid From
None		